A model was developed to describe the thermal response of large plastic bioreactors in incubators with variable air speed, and then used to provide a general guide for incubator design.

Reprinted from
PHARMACEUTICAL ENGINEERING®
The Official Journal of ISPE
January/February 2003, Vol. 23 No. 1

Incubator Design for Optimal Heat Transfer and Temperature Control in Plastic Bioreactors

by William Adams, Colette Ranucci, Sara Diffenbach, Kim Dezura, Charles Goochee, Abraham Shamir, and Scott Reynolds

Margaret Stava
margaret@biopharmequip.com
(562) 355-5859

Chambers, Walk-In Rooms
Scaleable Adherent-Cell Manufacturing Platform with Closed, Automated Cell Harvesting

Culture of mammalian cells for the manufacture of vaccines for human use has traditionally been performed in small plastic bioreactors such as T-flasks and roller bottles. Generally, the reactors are manipulated at ambient temperature for process operations such as cell plant, refeed, or infection. Subsequently, the reactors are transferred into incubators which warm and then maintain the cells at the optimal temperature for cell growth or viral propagation (e.g., ~37°C for human cell lines). The incubators are generally designed to control temperature using forced air circulation, and may range in size from a small tabletop unit to full walk-in rooms capable of storing thousands of reactors. To achieve process consistency and control, the time required for warming to optimal temperature must be satisfactory relative to the time scale of biologically significant events in the reactor, such as cell settling and attachment, initiation of growth, or viral transmission.

In recent years, the design of bioreactors has advanced in two ways. Firstly, to provide greater cell culture surface area within a given manufacturing footprint, and secondly to reduce the number of container openings and thereby provide increased sterility assurance. In so doing, however, it is apparent that the heat transfer necessary to provide the desired warming rates has become a bigger challenge. Table A shows the impact of design on the ratio of heat transfer surface area to cell culture area for several commercially available bioreactors, including the 40-tray Nunc Cell Factories (NCFs) reactors studied in this work.

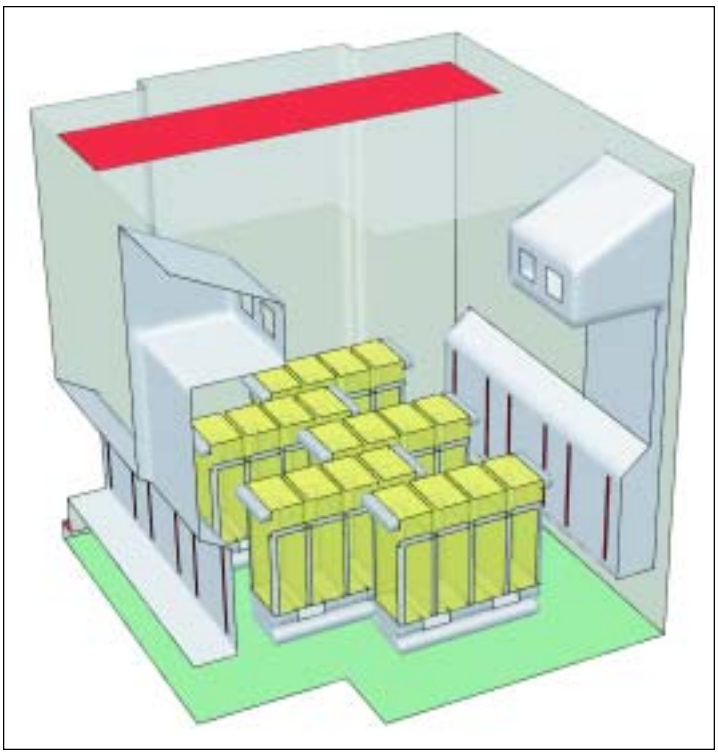

Figure 1. Isometric view of incubator layout and typical load pattern.

These design properties suggest that heat transfer into the 40-tray units will be ~10 times slower than into a T-flask if all other factors are equivalent.

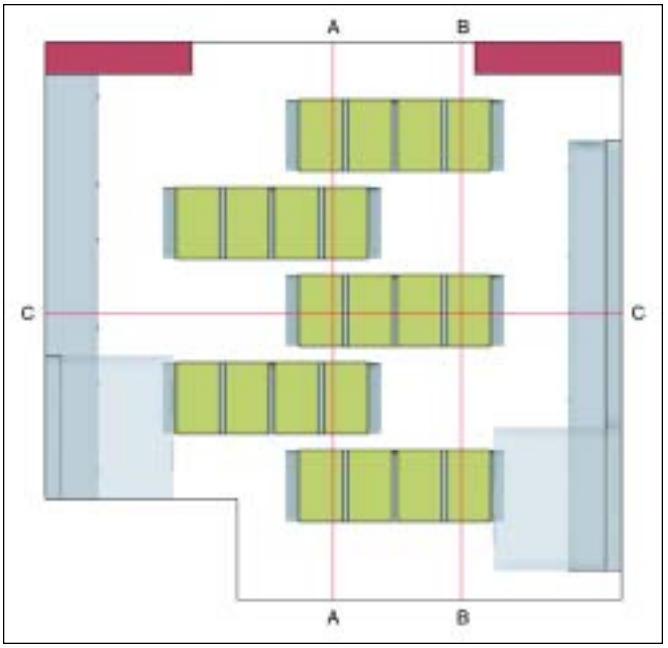

Figure 2. NCF load pattern and numbering key plan.

While the impact of warming rates has been shown to be important in some applications of cell and virus cultivation, heat transfer and temperature control of the largest reactor listed in Table A has not been well understood. Standard incubator designs generally promote heat transfer by recirculating air controlled at a specific temperature set point. Air speed and direction have essentially been driven by cGMP design factors rather than rigorous thermal performance analysis. To provide a class 10,000 environment, for example, walk-in incubators would generally be designed to provide HEPA-filtered airflow from the ceiling into the room with low wall returns to the HVAC system, typically at a minimum of 35 air changes per hour. Achieving a consistent warming time among bioreactors having very different surface area to volume ratios; however, will require different specific incubator airflow conditions.

The focus of this work was to analyze the transient thermal characteristics of 40-tray NCFs to determine the dependence of warming rates on airflow conditions in incubators. The results of this study were then generalized to facilitate incubator design and operation to enable optimal bioreactor performance and process robustness. More specifically, this article describes an experimental approach to assess the thermal response of 40-tray NCFs in walk-in incubators along with the development and use of Computational Fluid Dynamics (CFD) to model the thermal behavior, considering both steady state (fixed temperature) and transient (warming) modes. The utility of the model was to:

1. calculate air velocity and direction around the NCFs as a function of incubator design features

2. provide the lumped transient thermal model parameters for the NCFs that produce the same predicted transient response as measured data

Bioreactor Type	Cell Growth Area cm^2	Heat Transfer Area cm^2	Ratio
T-flask	175	546	3.1
Roller Bottle	850	1,050	1.2
NCF (2-tray)	1,264	1,741	1.4
NCF (40-tray)	25,280	8,718	0.36

Table A. Relative heat transfer considerations.

3. define the impact of air flow conditions on NCF warming rates in a general way to facilitate future incubator design optimization

Experimental and Computational Methods

Temperature Mapping in NCFs

The 40-tray polystyrene NCFs were positioned in sets of four on the stainless steel carts used for automated cell culture manipulations. Small holes were drilled in the sidewalls of selected trays to allow for the insertion of thermocouples. The tubing assemblies for vent and plant operations were placed into the applicable ports of each NCF, and the NCFs were filled with 0.33 mL/cm^2 of Water-For-Injection (WFI) (equivalent to 210 ml per tray). Thermocouples were inserted midway into the selected trays, manipulated until the end of each thermocouple was submerged in water, and subsequently taped in place to prevent inadvertent displacement during the mapping study. The temperature of up to 20 thermocouples available for use per mapping was monitored and recorded using standard data logging software. The thermocouples were calibrated pre- and post-use to ensure accurate data acquisition. The NCF carts were maintained at room temperature in an attempt to provide a uniform temperature for all trays. To start the experimental mappings, the carts containing the NCFs were wheeled into the 37°C incubator, and temperature data was then collected at five-minute intervals from each of the thermocouples. Temperature mapping studies were typically continued until all trays reached within 0.5°C of the 37°C incubator control set point. The data was transferred to spreadsheets for numerical and graphical analysis.

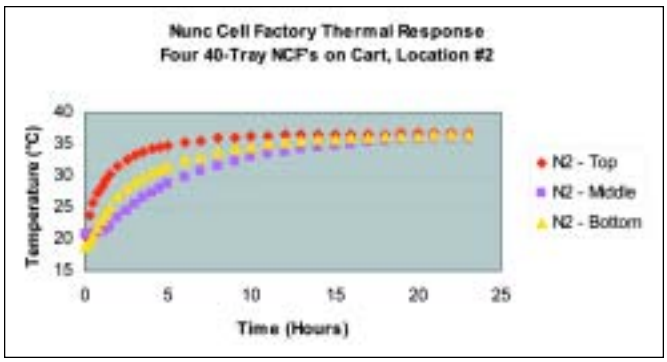

Figure 3. NCF thermal response at low air speed. Average local air speed ~28 FPM. Side wall air circulation units providing 0 FPM at supply slot inlets (off).

NCF Number and Layer	Time to Within 1°C (hours)
Cart1-N2-Top	7.1
Cart1-N2-Middle	19.0
Cart1-N2-Bottom	14.0

Table B. Thermal response time for trays at low air speed.

NCF Number and Layer	Time to Within 1°C (hours)
Cart5-N4-Top	5.0
Cart5-N4-Middle	9.0
Cart5-N4-Bottom	6.5

Table C. Thermal response time for trays at higher air speed.

Incubator Design Features

Two different-sized walk-in incubators were evaluated in the study. The first incubator was 9 ft wide by 9 ft long with overhead HEPA-filtered air supplied at ~1240 CFM (cubic feet per minute) at 37°C. Typically, five NCF carts, each holding four 40-tray NCFs, were placed in the incubators. Two low wall air returns were located along one wall. The second incubator measured 20.6 ft long by 9.8 ft wide with overhead HEPA-filtered air supplied at ~2,400 CFM and 37°C, and with low wall returns positioned at each corner of the room (four total). The bulk average air velocity in the middle of the incubators resulting from these supply and return arrangements was about 15 feet per minute (FPM). Both incubators had a stainless steel interior finish with well insulated wall panels. To provide for a wide range of air velocities in the vicinity of the NCFs, additional wall-mounted air recirculation units were installed. The fans in these units drew air in at an elevation of ~7 ft and drove it through a bank of 2 ft by 2 ft HEPA filters positioned at the level of the NCFs (approximately 1.1 ft to 3.1 ft above the floor). The flow from the filters was forced through slots about 0.08 ft wide by 1.8 ft tall (positioned about 1.2 ft apart), through which the velocity was increased. The output of the fans was designed to provide an air speed of up to ~1,000 ft per minute (FPM) at the slot outlet. By adjusting the output of the fan-powered recirculation units, the air speed in the vicinity of the NCFs could be significantly varied. Volumetric air flow rates were measured using standard portable flow hoods, and local air velocities were measured using a hand-held hot wire anemometer.

Computational Fluid Dynamics Modeling

The two incubator designs were modeled using Computational Fluid Dynamics (CFD). Large-scale three-dimensional CFD models were created from the physical domains described in the previous section. These models were built using commercially available general purpose CFD software. Parameters used for the model included the following: an unstructured solver, k-ε RNG turbulence capabilities, and a domain descretized with tetrahedral cells throughout. Approximately 620,000 computational cells (small incubator) and 910,000 cells (large incubator) were employed to solve for the three velocity directions, two turbulence terms, one pressure term, and one energy term.

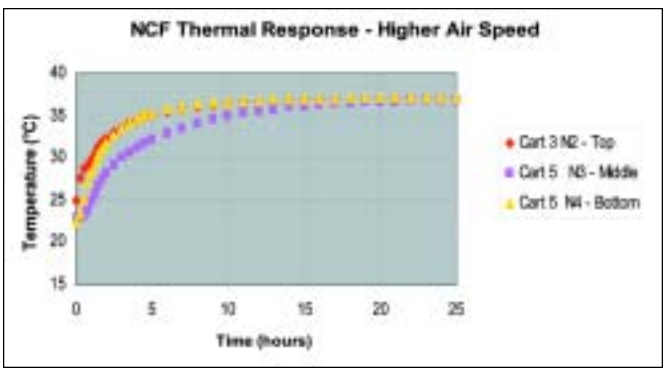

Figure 4. NCF thermal response at higher air speed. Average local air speed ~ 40 FPM. Side wall air circulation units providing ~ 550 FPM at supply slot inlets.

Experimental Results

More than 30 distinct temperature mappings of NCF warming were performed covering various NCF locations, airflow speeds, and directional patterns. An isometric view of the small incubator with five NCF carts is shown in Figure 1. A typical experimental load pattern along with the numbering scheme for carts and specific NCFs on each cart is indicated in Figure 2. The bulk average thermal performance of the 40-tray NCFs on the carts in low air flow conditions is shown in Figure 3 which shows the temperature versus time profiles for the top, middle, and bottom trays (numbers 1, 20, and 40 respectively). The data was taken from NCF #2 among the four on cart #1 (identifying nomenclature Cart1-N2). All trays exhibit the expected first order dependence on the difference between the tray and incubator temperature. The response is notably asymmetric; however, with the top tray warming the fastest, the bottom tray notably slower, and the middle tray warming the slowest following an initial lag phase. This pattern in the relative thermal response for the different trays was observed in all studies although the specific response times and magnitude of disparity between trays was influenced by airflow and heat transfer conditions.

To summarize the performance in a way most meaningful to the cell and virus cultivation, we evaluated the time to reach a temperature within 1°C of the incubator control point. Referring to the data in Figure 3, the performance is summarized in Table B.

For this experiment, the incubator temperature was 36.7°C, and the times listed above therefore represent the time to achieve 35.7°C. Within a group of experimentally mapped NCFs, the response time of comparable trays could vary by a few hours. The standard deviation (σ) in time required to reach within 1°C of the control temperature ranged from ~three hours for top trays to ~six hours for the slowest responding middle trays.

Representative performance within the incubator at higher air speed conditions is shown in Figure 4 which plots the temperature versus time profiles for the top, middle, and bottom trays from Cart 5-N4 in the load pattern. In this case, the sidewall air circulation units were providing ~550 FPM at

"Therefore, CFD was deemed as the more accurate and convenient means to solve the transient response problem as long as suitable values for R and C could be estimated."

the supply slot outlets. Although the NCF trays warm more rapidly in the higher air flow conditions, the asymmetric trend in response between trays remains prevalent. The response times can be summarized in Table C.

The faster response and reduced absolute deviation between layers would be expected to provide improved consistency and control of the cell culture.

The asymmetric thermal response between top and bottom layers in the 40 tray NCFs is in contrast to performance in the smaller two tray and 10 tray NCFs. In the 10-tray bioreactor, for example, both top and bottom trays lead the response of the middle tray by an equivalent margin. Apparently the cart used to support the 40 tray NCFs provides a significant additional heat capacity and thermal resistance. Interestingly, there was not any significant difference between the NCFs at different positions on the carts. That is the performance was essentially the same between the outside and inside positions (i.e. positions #1 through #4 are all similar). This was determined through analysis of variance applied to all the data from studies covering all positions in the load patterns. Warming rates were not significantly affected by cart location within the incubators studied, most likely due to the similar proximity of carts to airflow sources.

Modeling and Discussion of Results

The CFD models were first used to calculate air velocities

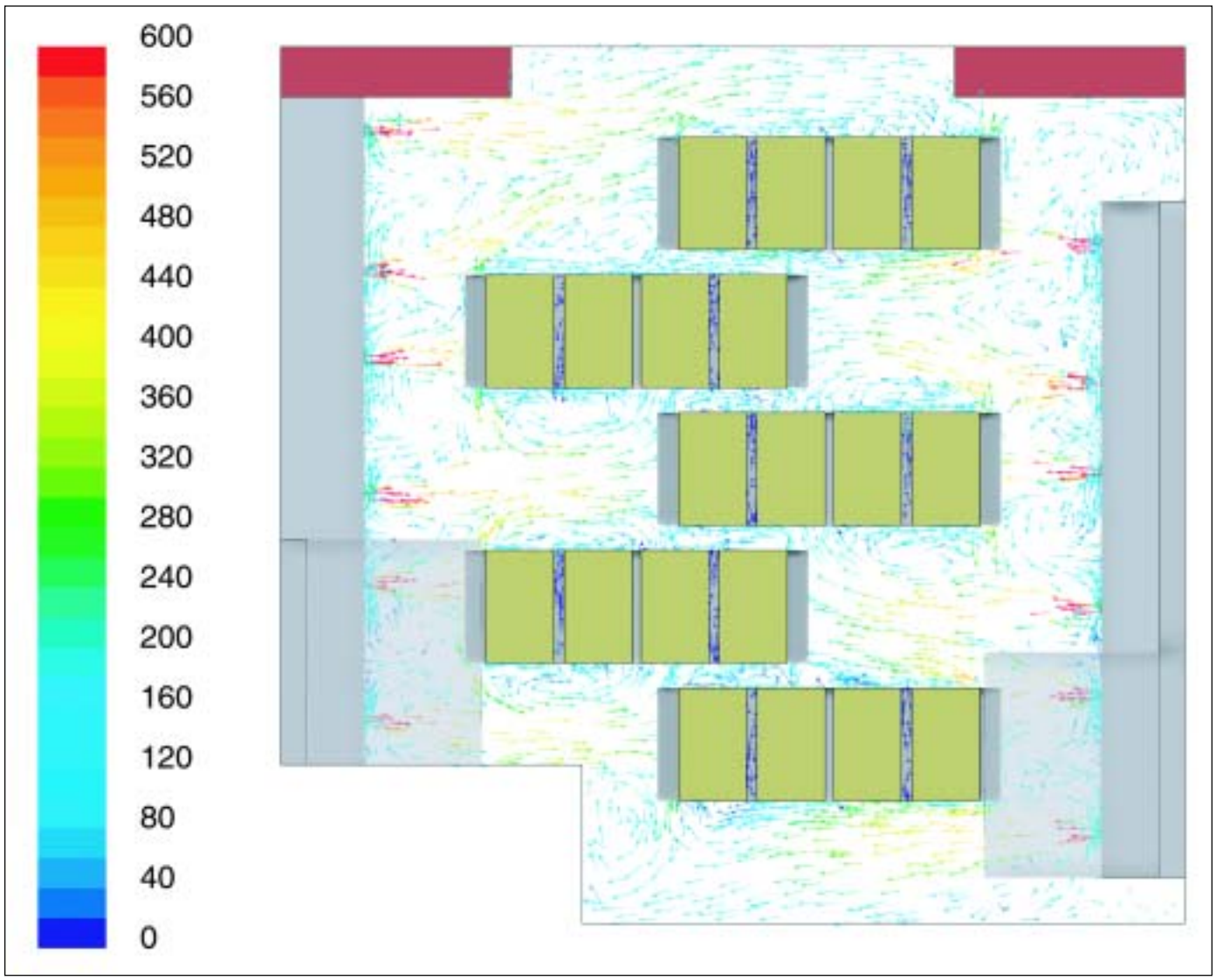

Figure 5. Plan view of velocity vectors in FPM - small incubator at 2.25 ft above floor.

throughout the incubators as a function of air speed settings for the wall-mounted recirculation units. Figure 5 shows a plan view of the predicted velocities at a distance of 2.25 feet above the floor. Upon entry into the room from the sidewall slots, the velocity vectors show a decline from the initial ~1,000 FPM with distance into the room and from impact with the cart obstructions. The areas in between NCFs on any given cart are slightly less than an inch apart and therefore retain relatively low air speeds for the orientation shown. Figure 6 shows a side-view of the same case, highlighting the high local velocities around the NCFs, the relatively lower velocities elsewhere, and the overall air circulation patterns throughout the room.

It was generally desired to isolate a closed-form function relating temperature rise time to various known physical parameters and boundary conditions. By identifying this function, a separate CFD simulation would not be required each time an incubator was designed. From standard transient heat transfer relationships, it was felt that the following equation could be used as a first order approximation:

Air Velocity Avg per slot (FPM)	Bottom trays (hrs)	Middle trays (hrs)	Top trays (hrs)
0	15.5	16.5	9.5
500	6.5	8.5	6.3
1000	4.8	6.8	4.8

Table D. Average time to within 1°C of incubator temperature.

$$T_{nunc} = (T_i - T_\infty)\, e^{-t/RC} + T_\infty \quad (1)$$

where:

T_{nunc} = Transient Nunc Cell Factory temperature

T_i = Initial Nunc temperature (nominally 18°C)

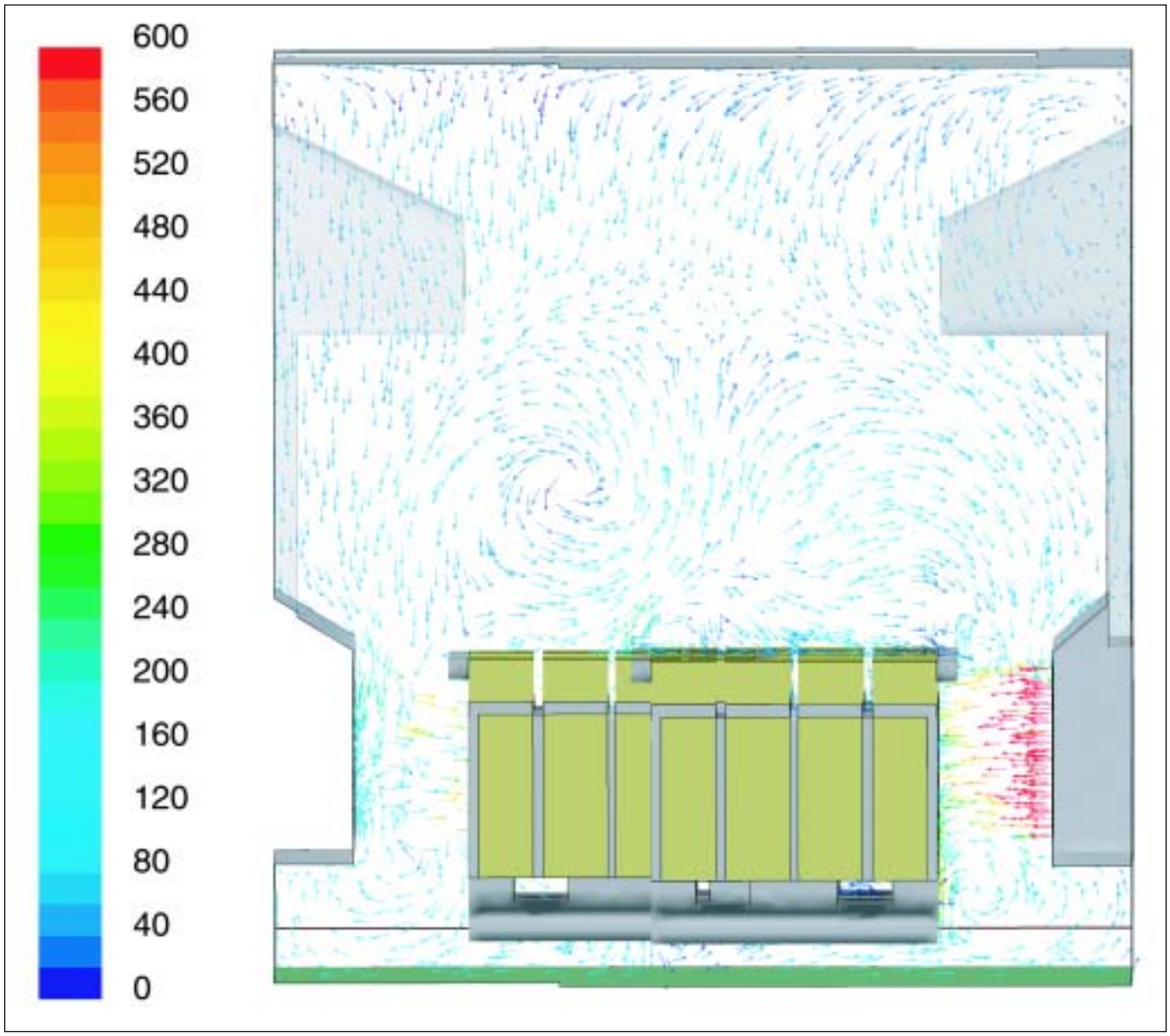

Figure 6. Side view of velocity vectors in FPM - small incubator.

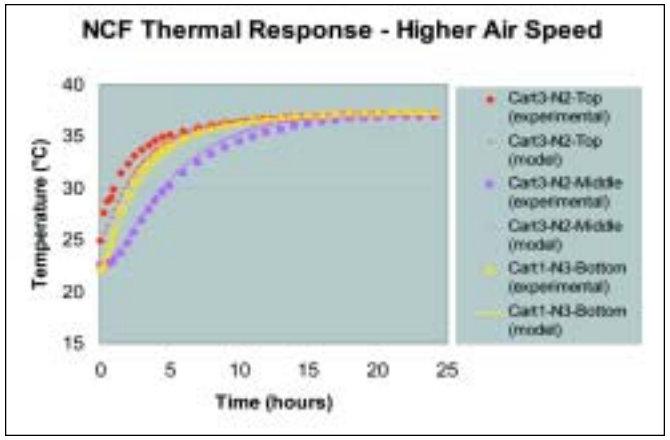

Figure 7. Comparison of model-predicted temperature rise to experimental measurements of a similar incubator layout at high airflow conditions (wall units at ~550 FPM).

T_∞ = Incubator bulk air temperature (37°C)
t = Time (seconds)
R = Thermal Resistance (1/hA)
C = Thermal Capacitance ($\rho C_p V$)
C_p = Specific Heat
ρ = Density
V = volume
h = Heat transfer coefficient
A = Surface area

Initially, it was believed that the parameters of equivalent thermal resistance and thermal capacitance could be directly determined using calculated values for surface areas, volumes, densities, conductivities, specific heats, and heat transfer coefficients for the carts and bioreactors. However, many attempts at solving the function revealed that the relationship was more complex with a strong dependence on other factors such as local airflow velocities, cart orientation, etc. Therefore, CFD was deemed as the more accurate and convenient means to solve the transient response problem as long as suitable values for R and C could be estimated. Along these lines, several transient CFD models were run using closed-form thermal property calculations (to calculate values for R and C), but all such simulations failed to adequately describe the measured transient response of the Nuncs.

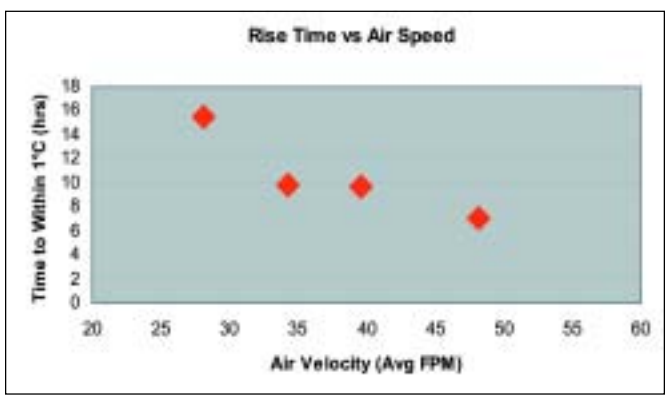

Figure 8. Correlation between NCF warming time and local average air velocity.

After the above technique failed to produce the desired results, an attempt to iteratively "back-calculate" the R and C parameters was made as follows. From the steady state CFD simulation, the heat transfer coefficients were calculated as were the bulk air temperature and the initial NCF layer temperatures. A two-variable least square fit for R and C was made using a power function developed from the experimental data acquired for various air flow rates. This equation used the known variables of temperature and time to provide the best fit values for R and C. These values were then used in a CFD transient model to predict the comprehensive temperature response behavior of the Nuncs. This procedure was further repeated until the calculated thermal resistance and capacitance provided a good emulation of the experimental data for the low air velocity case. Model predictions for the time to reach within 1°C of the incubator control point agreed with experimental data to within two hours for all such cases.

The model was then challenged to predict warming rates under distinctly different air flow conditions. Such an assessment is exhibited in Figure 7 which shows both experimental and predicted thermal response curves for the case in which air flow from the side wall units provides ~550 FPM at the HEPA filter outlet slots. There are three sets of data shown for this faster warming case, corresponding to three representative tray mapping locations among the overall load pattern of five carts containing 20 NCFs. In Figure 7, the dashed lines show the model-predicted temperatures relative to the actual experimental values. Agreement is good in general, the predicted times to reach within 1°C are accurate to within two hours.

The model was used similarly to predict warming rates at three different air flow conditions. The thermal response of the NCFs as a function of the nominal side wall air velocity can be summarized in Table D.

The times listed are average response times for all sample points on the indicated tray location (the model allowed for a total of 11 such points). Table D shows that air speed has less impact on the top trays which have relatively high exposed surface area. The bottom or middle trays have smaller exposed surface areas which leads to a stronger dependence on changes to the heat transfer coefficient.

Incubator Design Guide

An important potential use of this heat transfer analysis and NCF thermal response modeling is to facilitate incubator design. Ideally, incubators could be designed for reliable, predictable performance without the need for developing and running a detailed computer model of thermal response for NCFs (or other bioreactors) in each specific incubator geometry and load pattern. Along those lines, we sought to generalize the model results to enable prediction of NCF warming rates as a function of local average air speed.

More specifically, we developed a correlation for the NCF warming time as a function of the average air velocity which can be experimentally measured and is a physically intuitive parameter. Average air velocities were calculated by the CFD simulation program for the different side-wall velocity cases. The average was calculated by sampling 120 point locations

around the NCF carts. These points were regularly spaced, 2 inches away from the carts, covering the top, middle, and bottom zones of each NCF, along both the long and short sides of the cart. The resulting data for all tray locations was then plotted in Figure 8 as time to achieve 36°C (average time for all trays) versus the average local air speed in FPM. The plot clearly shows a steep decline in warming time between low air speed of ~28 FPM and the more moderate speed of ~48 FPM with a slower decline expected beyond that. The step like appearance in the middle of the plot is believed to be driven by a transition from the laminar to the turbulent flow regime. Figure 8 suggests that reasonably rapid thermal response as well as effective temperature consistency and control will be provided from an incubator environment designed to provide average local air speeds of at least 35 FPM. Note that much higher local point velocities may be needed to achieve an average surrounding velocity of 35 FPM because other areas may be relatively stagnant.

Higher air speeds generally dictate larger air handlers and proportionally greater surface area of HEPA filters since the absolute air speed through the filters should be less than ~100 FPM. As a result, higher incubator air flows will always be more costly to install and operate. The most economical approach to achieve higher local air velocity is to position the dominant room air flow drivers, such as the main supply inlets and/or returns, as close to the bioreactors as is practical. Higher local velocities may require the use of ductwork to provide post-filtration air flow convergence to achieve the desired minimum air speed at important locations in the load pattern. Reasonably rapid and consistent bioreactor warming rates can be achieved through such incubator design approaches.

Conclusion

Incubator air speed was observed to have a significant impact on the warming rate of large plastic bioreactors commonly used for cell and virus cultivation. The relationship between thermal response and air velocity was well correlated through the use of a model utilizing computational flow dynamics. Application of the model indicated that average local velocities in excess of 35 feet per minute were required to achieve timely and consistent response.

Credits

1. 40-tray NCF bioreactors were Nunc Cell Factories procured from Nalge Nunc, Intl.

2. The CFD simulation software used was Fluent®, from Fluent, Inc.

About the Authors

William Adams received his PhD in chemical engineering from Cornell University with a minor in computer science. He joined Merck in 1990, and has progressed through positions in Technical Service, Operations Management, and is currently Associate Director in Vaccine Process Engineering. His current principal focus is on process equipment and facility design for live virus vaccines.

Merck & Co., Inc., WP60T-2, PO Box 4, Sumneytown Pike, West Point, PA 19486.

Colette Ranucci joined the Bioprocess Research and Development department within Merck Research Laboratories in 1992, shortly after receiving BS/BA degrees in chemical engineering and German. After working in the area of vaccine process development for several years, she returned to Rutgers University to complete the PhD program in chemical engineering. Since rejoining Merck in 2000, her primary responsibilities have included process development, scale-up, and process validation related activities. She is an active participant of the BIOT division of ACS, serving as the membership chair.

Merck & Co., Inc., WP17-201, PO Box 4, Sumneytown Pike, West Point, PA 19486.

Sara Diffenbach received a BS in chemical engineering from the Pennsylvania State University in 2000 and joined Merck & Co., Inc., as a staff engineer in the Viral Vaccine Technology and Engineering group, focusing on technology transfer and facility start-up. She recently joined Pfizer, Inc., as a Production Leader in the manufacturing of personal care products.

Pfizer, Inc., 400 W. Lincoln Ave., Lititz, PA 17543.

Kim Dezura is a Senior Process Engineer at Merck.

Merck & Co., Inc., WP62-7, PO Box 4, Sumneytown Pike, West Point, PA 19486.

Charles Goochee is a Director of Bioprocess R&D at Merck.

Merck & Co., WP17-201, PO Box 4, Sumneytown Pike, West Point, PA 19486.

Abraham Shamir joined Merck in 1989 and has held positions of increasing responsibility in technical operations and process engineering. After receiving a BS in biochemistry and a PhD in chemical engineering from Columbia University, he joined Schering-Plough where he progressed to the position of manager for large-scale recombinant protein purification. He went on to join BioTechnology General as director of protein purification - Process Development and Manufacturing.

Merck & Co., Inc., WP60T-2, PO Box 4, Sumneytown Pike, West Point, PA 19486.

Scott Reynolds is a Senior Engineer at Computer Aided Engineering Solutions.

Computer Aided Engineering Solutions, Division of Bearsch Compeau Knudson Architects and Engineers, PC, 41 Chenango St., Binghampton, NY 13901.